

Analysis of Overcurrent Protection for Topology Morphing LLC Converters by Diode Clamping applicable to EV chargers

Jiho. Kwak¹, Ki-Bum. Park¹, and In Gwun. Jang¹

¹ Korea Advanced Institute of Science and Technology (KAIST), Republic of Korea

Abstract-- Recently, EVs (Electric Vehicles) increased their pack voltage from 400V to 800V. It has shortened the charging time, but EVs with 800V now have to carry an extra boost converter with their OBCs (onboard chargers) since most fast chargers support only 400V systems. This consumes extra weight and volume from EVs. Therefore, chargers need to handle both 400V and 800V systems to make EVs more competitive in the market. However, the chargers' efficiency will decrease due to the broader expected output voltage range. As a solution, this paper suggests a Topology morphing technique. Nonetheless, the main scope of this paper is the overcurrent protection of such applications since there isn't much research about overcurrent protection schemes for topology morphing. This paper proposes diode clamping of a resonant capacitor in a capacitor-shared LLC converter applicable to EV chargers for overcurrent protection with simulation results.

Index Terms— Capacitor Sharing, Diode Clamping, Overcurrent Protection, Topology Morphing

NOMENCLATURE

C_r	Equivalent Resonant Capacitance
C_s, C_c	Resonant Capacitors
C_n	Capacitance Sharing Ratio
L_r	Resonant Inductor
L_m	Magnetizing Inductor
L_n	Inductance Ratio
R_{ld}	Load Resistance
S_1, S_2, S_3, S_4	Switches
D_1, D_2	Rectifying Diodes
Dc_1, Dc_2	Clamping Diodes
C_{o1}, C_{o2}	Output Ripple capacitor
f_{sw}	Switching Frequency
$I_{s,peak}$	Peak current through switches
V_{in}	Input Voltage
V_{out}	Output Voltage
$V_{out,rate}$	Maximum Rated Output Voltage
$V_{out,over}$	Output Voltage at Overcurrent
P_{rate}	Maximum Rated Power
P_{over}	Overpower Caused by Overcurrent
V_n	Normalized Output Voltage ($V_{out,over} / V_{out,rate}$)
P_n	Normalized Power (P_{over} / P_{rate})

J. INTRODUCTION

There has been a global effort to reduce CO₂ emission [1]. Since automobiles take a big part in CO₂ emissions, the effort boosted the development of EVs and rapidly took meaningful shares in the automobile market. However, there seem to be many difficulties to overcome in the further transition to EVs from fossil-fueled vehicles. One of the speed bumps that slows down the growth of EVs in the market is the charging speed. The charging time for EVs is generally incomparably longer than the time it takes

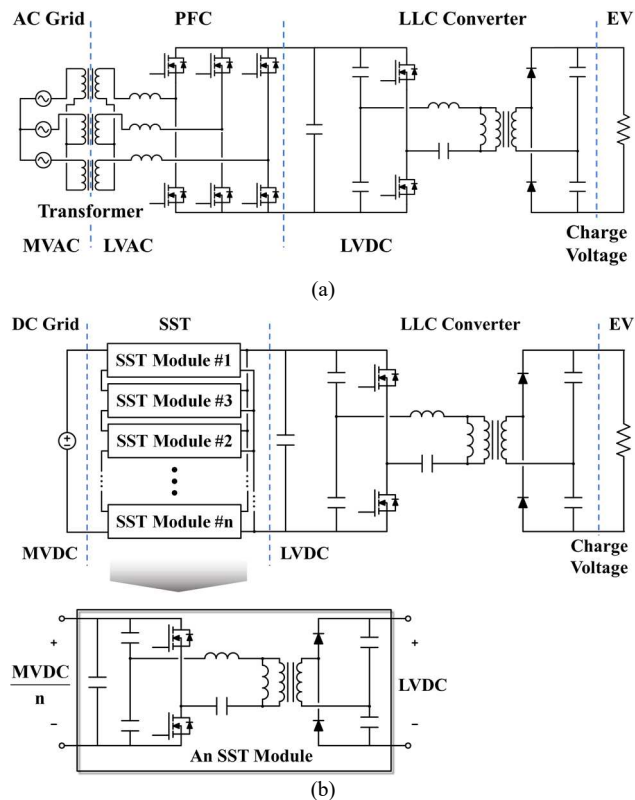


Fig. 1. A configuration of a DC fast chargers for EVs considering (a) Charging system from the AC power grid, and (b) Charging system from the DC power grid

to fill up a gas tank in a fossil-fueled vehicle. Fortunately, the recent DC fast charging infrastructure reduced the charging time to under an hour. Unlike previous EV chargers, DC fast chargers don't require any extra equipment such as inverters or rectifiers and also OBCs from EVs. The chargers provide compatible DC power that can directly connect to the EVs' battery pack. The Tesla superchargers are good examples [2], [3]. Not only they can be spatially more efficient, but the supplying current can be also increased greatly because the chargers don't need to consider the rated power of the extra equipment. The overall configuration of the considered DC fast charger is shown in Fig. 1. The one downside is that these chargers require a high-power PFC and a transformer as shown in Fig. 1(a). However, in the future, the ongoing growth in the DC power grid can take over the AC power grid. Then, this charging system can be even more attractive with solid state transformers (SSTs) as shown in Fig. 1(b). SSTs can reduce the size of the power substation by eliminating the huge transformer and the PFC. Also, it

transmits the DC power directly to the chargers. The DC transmission is known to be more efficient than AC transmission in the future grid system as well [4].

The effort of minimizing the charging time was not only done in chargers but also in EVs themselves as well. Automakers made their battery packs in EVs with higher voltage and higher power. Most fully electrified vehicles were equipped with 400V battery packs but, EVs with 800V battery packs begin to appear in the market recently [5], [6]. Twice of power can be delivered with the same current. The problem is that since DC fast chargers are designed for a 400V battery pack, these chargers are not directly compatible with the 800V battery pack. Therefore, EVs require extra boost converters to bump up the charging voltage. Since the boost converters have to deal with high power, the weight and volume have to be heavier and larger. Considering EVs are built for transportation, such an extra system can be inefficient. Thus, DC chargers must consider both 400V and 800V systems to enhance the growth of EVs in the market by eliminating these extra boost converters. If chargers consider both 400V and 800V, the chargers have to bear with the downside. A broader expected output range of converters in chargers will lose more efficiency.

In this case, Topology morphing can come in handy. Topology morphing uses two switching modes to cover a broader gain range [7]. Hence, this paper explains a Topology morphing converter applicable to DC fast chargers for better efficiency. The operation of Topology morphing will be further explained in section 2. However, this paper's scope is not about the Topology morphing itself but the protection of such application. It is because there is much research about Topology morphing [8], [9] but, not much research about its protection. There have been many accidents while charging EVs all around the world. When accidents happen Li-ion battery pack usually burns inextinguishably leaving nothing behind to investigate. Despite this, few accidents indicate that there were short circuit problems that caused the accident [10]. The short circuit ends up in excessive overcurrent that can harm power semiconductors and other components in the charger. Considering it, in this paper, analysis of the diode clamping overcurrent protection method for Topology morphing LLC converters that can be applied to DC fast chargers is investigated.

II. TOPOLOGY MORPHING

An LLC converter was chosen as a DC fast charger topology in this paper because it can operate in comparably high frequency due to its ZVS ability. Thus, the converters can have a comparably higher power density. Such advantages allowed LLC converters to be applied in many different areas already [11] ~ [13]. Since DC fast chargers are usually located in parking lots, shopping centers, hotels, restaurants, etc... [5], power density is a critical issue for the EV charging application as well. However, with a broad range of gain conditions, the efficiency of LLC converters can be limited.

To address this limitation, 'Topology morphing' which dynamically reconfigures the topology of the converter by

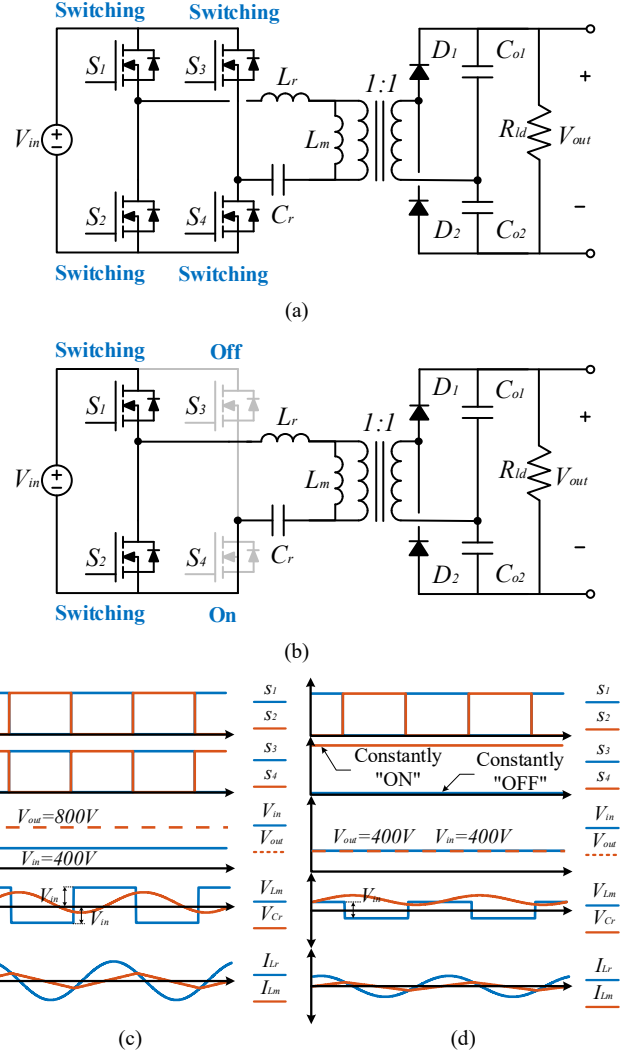
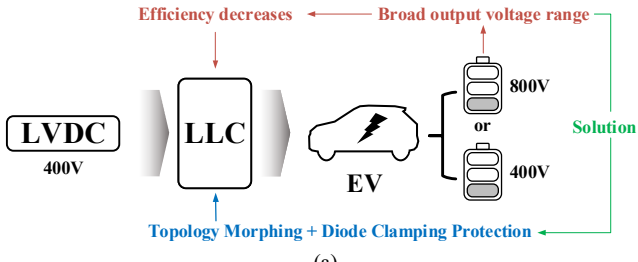
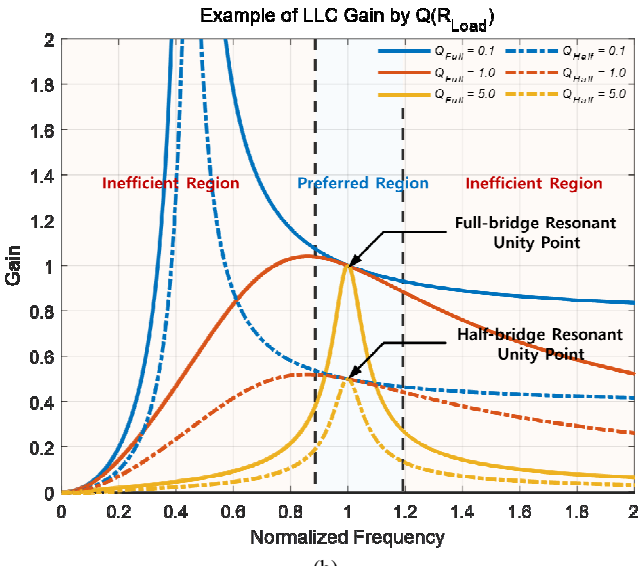


Fig. 2. An explanation of Topology Morphing (a) Circuit diagram of full-bridge mode operation, (b) Circuit diagram of half-bridge mode operation, (c) Waves of full-bridge mode operation, and (d) Waves of half-bridge mode operation

morphing switching modes can be applied. Topology morphing can improve the converter's efficiency under two different operating gain points. In EV chargers' case, 400V and 800V output voltage would be the two output points. There are two different switching modes in topology morphing: Full-bridge mode and half-bridge mode as shown in Fig. 2. A full-bridge mode operates in regular switching operation of the full-bridge inverter from LLC converters. As shown in Fig. 2(c), S_1 and S_4 switch alternately to S_2 and S_3 . Therefore, the input voltage is applied alternately (positively and negatively) to the resonant inductor L_r . Hence, the output voltage becomes doubled from the input voltage at the resonant frequency with the voltage doubler attached in Fig. 2(a). In the EV chargers' case, the full bridge mode can charge EVs with 800V battery packs as a load from 400V LVDC as in Fig. 3(a). The LVDC is set as a 400V system because it was found to be the most suitable voltage from the previous research [14]. Morphing such a configuration would yield the half-bridge mode operation. When only switching S_1 and S_4 alternately while S_3 stays constantly off and S_2 stays constantly on, the inverter becomes identical to the half-



(a)



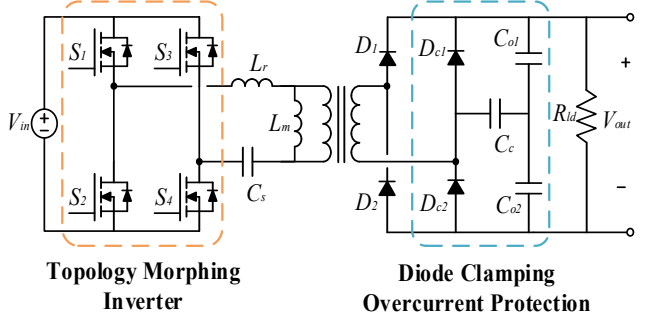
(b)

Fig. 3. Advantage of Topology morphing (a) Proposed concept of Topology morphing EV charger with protection, and (b) Gain curves

bridge configuration as shown in Fig. 2(b) and (d). Then, the input voltage and 0 voltage are applied to the L_r alternately. As a result, the same amount of input voltage is applied to the output at the resonant frequency with a voltage doubler as shown in Fig. 2(d). Again, in the EV chargers' case, half bridge mode will be charging EVs with 400V battery packs from 400V LVDC as in Fig. 3(a). In sum, by Topology morphing, the chargers will easily cover both 800V and 400V battery pack systems with minimum loss in efficiency.

The effectiveness of Topology morphing in sense of improving efficiency is shown more detailly in Fig. 3(b). Solid lines represent the full-bridge switching mode and dotted lines represent the half-bridge switching mode. In the preferred operating frequency region which is defined as the vicinity of resonant frequency, there exist two different gain curves for various load conditions represented as quality factor, Q . The usual LLC converters would have only solid lines. Since Topology morphing utilizes both of these gain curves, the switching frequency doesn't need to move far away from the resonant frequency to meet the gain condition. This helps because if the switching frequency moves too high the switching loss causes low efficiency and if the switching frequency moves too low the lost ZVS causes low efficiency.

Moreover, if this Topology morphing LLC converter can have a protection mechanism inherited without any additional protection device as shown in Fig. 3(a), the spatial advantage would be even greater without any additional overcurrent protection devices.



Topology Morphing

Inverter

Diode Clamping

Overcurrent Protection

Fig. 4. A proposed protective topology morphing circuit

III. CAPACITOR SHARING AND DIODE CLAMPING

As mentioned before, there are not many clear investigations of the accidents that occurred while charging the EVs in the DC fast charging stations. However, there are few investigations that indicate that accidents are caused by internal short circuit problems in EVs [10]. A short circuit creates an excessive amount of overcurrent which results in faults in the power system. Thus, it is important to note that all EV chargers must have overcurrent capability. There are a few protection methods to prevent overcurrent as in [15] and [16], but the diode clamping method seems to be the most suitable one for EV chargers. Since EV chargers deal with such a large capacity of current, overcurrent for just a small amount of time can do severe damage to the power system. Thus, the response time for the protection method must be as quick as possible. Since the diode clamping method has inherited protection components within the circuit, the response for the overcurrent is theoretically instant. However, there's not much research (if there's any) about the overcurrent protection method of LLC converters with Topology morphing using the diode clamping method.

Since Topology morphing takes place on the primary side of the converter, it is simpler to apply the diode clamping on the secondary side. Also, it is difficult to apply the diode clamping method to the full-bridge operation. There was some previous research that tried the diode clamping method on the secondary side of the resonant converter [17]. However, there's a problem with itself applying the diode clamping method on the secondary side of the converter. The resonant capacitor must be present on the primary side of the converter to eliminate the DC component in half-bridge mode operation. Thus, the capacitor sharing method introduced in [18] is adopted. Two series connected resonant capacitors are located divided by a transformer: C_s on the primary side and C_c on the secondary. This way, diode clamping can be done in full-bridge mode operation through C_c , and resonant capacitor C_s can compensate for the resonance in half-bridge mode operation. The proposed circuit diagram is shown in Fig. 4. As shown in Fig. 4. The C_c is clamped by D_{cl} and D_{c2} , whenever it obtains more voltage than the half of output voltage as shown in Fig. 5. The interesting part is that the intensity of overcurrent protection is determined by the size of C_c . The size of C_c can be varied as well as C_s . They are determined by the normalized capacitance, C_n as shown in (1) and (2).

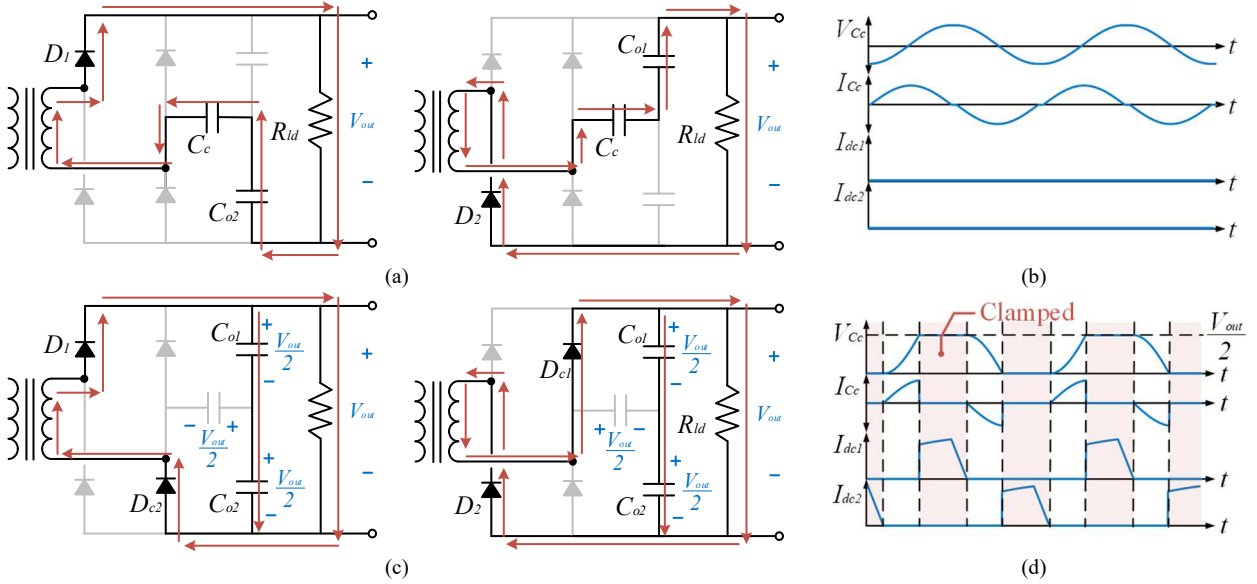


Fig. 5. An explanation of diode clamping (a) Circuit diagram under normal operation, (b) Waves under normal operation, (c) Circuit diagram under clamping operation, and (d) Circuit diagram under clamping operation

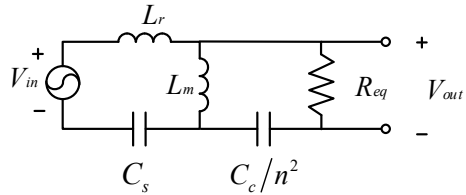


Fig. 6. An FHA model of a proposed circuit.

$$C_n = \frac{C_r}{C_s} \quad (1)$$

$$C_c = \frac{C_s C_r}{C_s - C_r} n^2 \quad (2)$$

When $C_n = 1$, there will be no clamping action, and when $C_n = 0$, the clamping capacity is at its maximum. The ratio C_n between 0 and 1 will determine the clamping intensity. However, half bridge operation in the case of $C_n = 0$ is impossible which makes it a non-suitable option. Note that the transformer's turn ratio is considered as 2 in Fig. 4 because of the voltage doubler. With bigger C_n , the LLC converter obtains a wider gain range, and with smaller C_n , better overcurrent protection capability. The reason why low C_n has more sensitive diode clamping capability is because of (3).

$$V_{c_e} = \frac{1}{C_c} \int i_{c_e} dt \quad (3)$$

The increment of voltage across the capacitor is inversely proportional to the capacitance of the capacitor. Since low C_n means smaller C_c , the diode clamping becomes much more sensitive in low C_n .

First harmonic approximation (FHA) modelling was applied for further investigation of this proposed capacitor sharing method. The FHA equivalent circuit of the proposed circuit in Fig. 4 is shown as Fig. 6. Notice that the transformer turn ratio n from C_c/n is set as 2 because of the voltage doubler. The voltage doubler increases the output voltage twice and thus the current at the same load

resistance. The FHA modeling was done through referencing [19] ~ [22]. The gain equation of the FHA model is shown in (4). The equation is simplified with letters A~F which are substitutable as (5).

$$\frac{V_{out}}{V_{in}} = \frac{-A\omega^3 i}{B + C\omega i - D\omega^2 - E\omega^3 i + F\omega^4} \quad (4)$$

$$A = 8n^2 R_{ld} L_m C_s C_c$$

$$B = \pi^2 n^2$$

$$C = 8n^2 R_{ld} C_c$$

$$D = (L_m + L_r) \pi^2 n^2 C_s + \pi^2 L_m C_c$$

$$E = (L_m + L_r) 8n^2 R_{ld} C_s C_c$$

$$F = \pi^2 L_r L_m C_s C_c$$

Using (4), An example of the gain curves by C_n at normalized power $P_n = 1$ is shown in Fig. 7(a). The inductor ratio L_n was set as 7 and the resonant frequency used for the normalized frequency F_n on x-axis is adopted by the resonant frequency of regular LLC converters as (6).

$$f_r = \frac{1}{2\pi\sqrt{L_r \cdot C_r}} \rightarrow F_n = \frac{f_{sw}}{f_r} \quad (6)$$

The example in Fig. 7 indicates the gain curves of a half bridge operation can be figured out by simply multiplying the half by the gain of a full bridge operation.

Notice how the converter gain decreases as C_n decreases. Also, the important thing to note is that there's no more unity point as a regular LLC converter which all gains from various load meet together [21]. In that matter, the characteristics of the converter is different from the regular LLC converters, worse if the C_n is lower. Also, because the characteristics changed there's a minor difference in ZVS condition as well. Thus, it is critical for users to see the gain curves first and heuristically chose the parameters of the converter through simulation. But, since the shape of the curve is not too different from the regular LLC converters, it will be a great choice to start designing as if the converter is a regular LLC converter initially.

Increasing the load current to $P_n = 10$ would result as

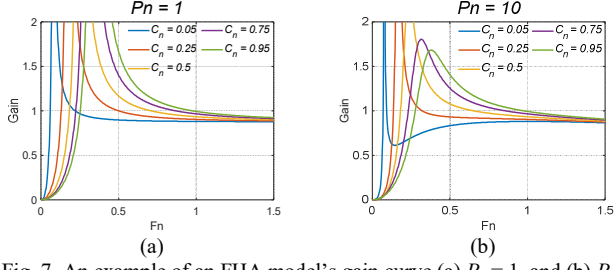


Fig. 7. An example of an FHA model's gain curve (a) $P_n = 1$, and (b) $P_n = 10$

Fig. 7(b). The gain quickly decreases and its intensity of decrement is larger as C_n decreases.

IV. SIMULATION

An example of designed EV charger with diode clamping topology is investigated through the simulation. The first thing to check is the current through switches. Switches made with silicon are usually vulnerable to high temperatures. Since switches that deal with high power are usually very expensive, it is important to minimize the damage to the switches. The excessive amount of current creates a high rise in temperature thus, it is important to check the switch current. Then the output voltage is checked. It will simply demonstrate how much voltage is limited by the clamping method. It is analyzed by the normalized output voltage V_n . From the simulation, the overcurrent is generated by decreasing the output load resistor, R_{ld} in Fig. 4 that creates the corresponding normalized power, P_n where $P_n = 1$ is a nominal power. The simulation follows the structure of Fig. 4 and the specification of the converter are $V_{in} = 400V$, $V_{out} = 800V$, $P_{rate} = 11kW$ for full bridge operation, $V_{out} = 400V$, $P_{rate} = 5.5kW$ for morphed half bridge operation. The switching frequency, f_{sw} is set as 100kHz and the parameters for other components are $L_r = 7.82\mu H$, $C_r = 323.98nF$, and $L_m = 54.73mH$.

Fig. 8 shows how the regular LLC converter reacts to the overcurrent with ten times of rated power. The peak current through switches at full bridge mode soars from about 36A to about 421A right away. Notice it's even higher in the transient response. The output voltage decreases a little bit as well because the Q changed and the output current also soars quickly. The trend seems about the same for both full bridge mode and half bridge mode. The only difference would be the output voltage. Fig. 9 shows the activated protection with various C_n under $P_n = 10$. Fig. 9(a) and (d) show the result when $C_n = 0.95$ which is almost the same as a regular LLC converter. Not much protection is done in this case and the voltage from C_c indicates that clamping capacitors didn't even work. However, at rated power, $C_n = 0.95$ showed a 0.7% of output voltage drop from the regular LLC converter's output voltage at rated power. It's because the gain curve is almost identical to the regular LLC converter as seen in Fig. 7. Fig. 9(c) and (f) on the other hand, show about a 12% difference in output voltage at rated power. Thus, if one chose $C_n = 0.05$, one must compensate the converter

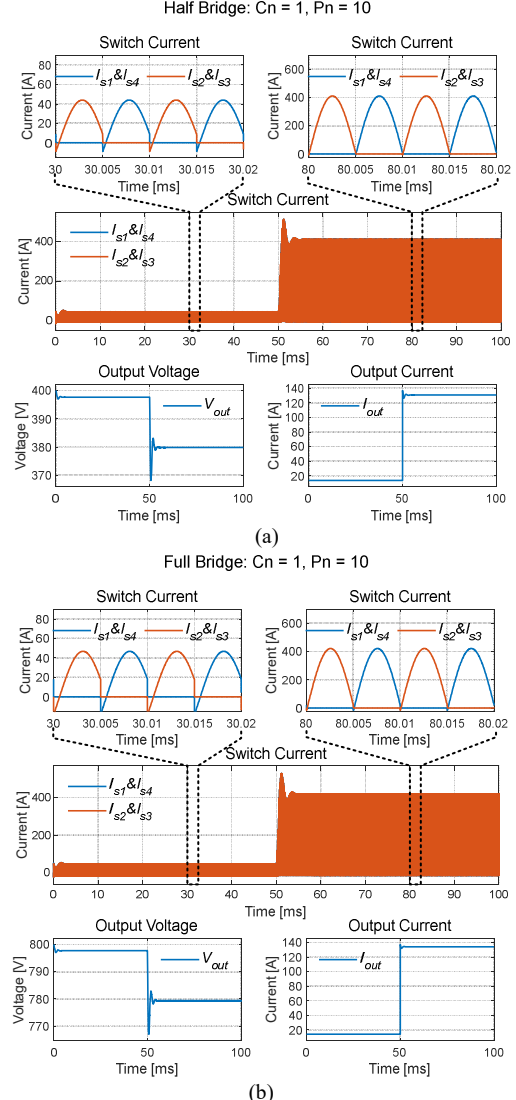


Fig. 8. Overcurrent at 50ms without protection at $P_n = 10$ (a) Full Bridge, and (b) Half Bridge

with V_{in} or transformer ratio. Despite this, to show the characteristics, this paper proceeded with simulation without compensation. The case of $C_n = 0.05$ shows absolutely superior protection performance though. There's no transient overshoot and the peak current through switches for full bridge mode is about only 97A compared to 421A with no protection. Notice from the voltage of C_c that clamping diodes strongly suppresses the overcurrent. Fig. 10 shows the peak current through switches by C_n and P_n . The protective effect is clear as C_n decreases.

The output voltage results of the simulation are shown in Fig. 11. It is clear to see that as C_n decreases; output voltage decreases rapidly. On the full bridge mode case, the normalized output voltage V_n was 0.39 with $C_n = 0.05$ at overcurrent with $P_n = 10$. Morphed half bridge case showed more significance with $V_n = 0.23$ with $C_n = 0.05$ at $P_n = 10$. If the sensors are fast enough, when the over current happens at 800V output, it can quickly morph to half bridge operation in emergency for further protection as well.

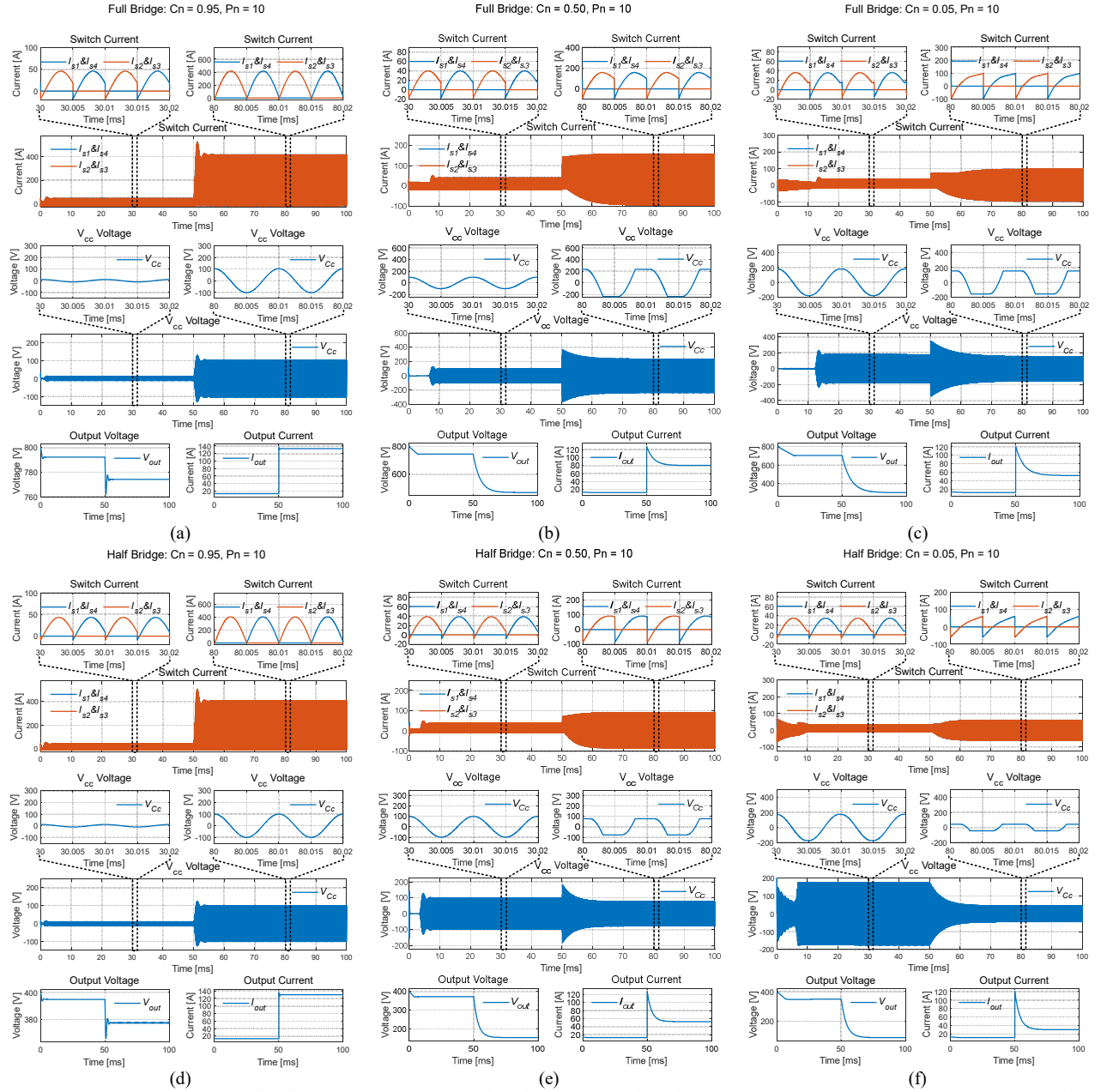


Fig. 9. Overcurrent at 50ms with different C_n at $P_n = 10$ (a) Full Bridge $C_n = 0.95$, (b) Full Bridge $C_n = 0.50$, (c) Full Bridge $C_n = 0.05$, (d) Half Bridge $C_n = 0.95$, (e) Half Bridge $C_n = 0.50$, and (f) Half Bridge $C_n = 0.05$,

V. CONCLUSION REMARKS AND FUTURE WORK

This paper investigated a diode clamping protection topology for an LLC converter that can be applied to EV chargers with both 400V and 800V systems. The topology worked well with both full-bridge and morphed half-bridge operations. Though bigger C_n provides better protection, it increases the size of the capacitor and narrows the gain range by changing the switching frequency [18]. Thus, if one has to have a wider gain range by changing frequency, lowering C_n too much will not be a good option. Also, since gain curves are changed a bit with low C_n , it has to be compensated through transformer ratio or V_{in} . Before using the proposed topology, one must optimize the C_n properly with one's interest whether it is the size of capacitors, gain range, protection, etc. So far,

this has to be done in a heuristic way. Therefore, in future work, such an optimization process can be investigated and the proposed circuit is going to be tested with a suitable hardware implementation.

Moreover, this Topology morphing method and protection scheme can be used in each module of an SST from Fig. 1(b). Then, not only the voltage can be more flexible but also each of these modules can have its own protection capability which can reduce the size of SSTs greatly. In the future, such an application can be considered for the DC grid system.

ACKNOWLEDGMENT

This research was supported by UNDERGROUND CITY OF THE FUTURE program funded by the Ministry of Science and ICT.

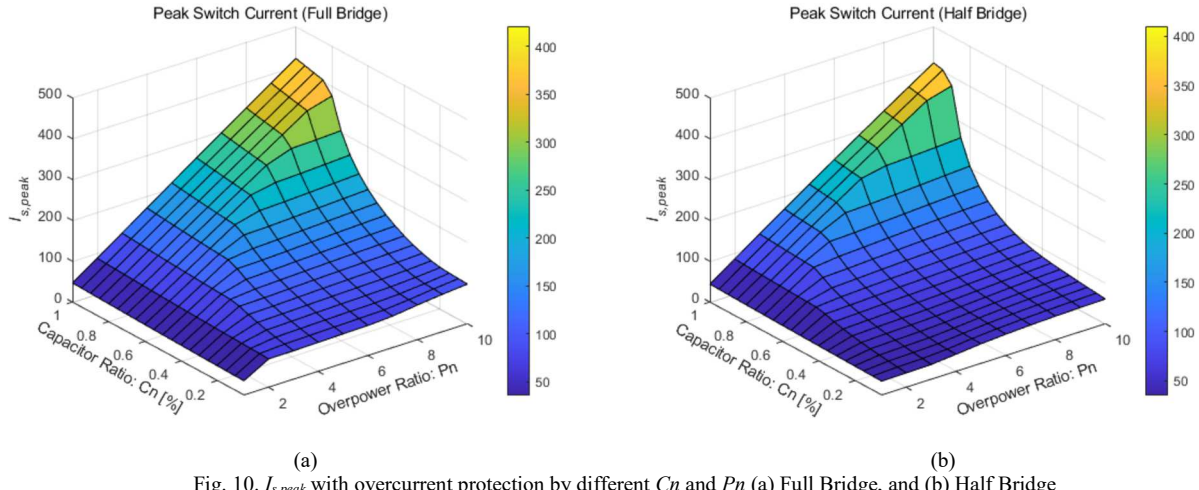


Fig. 10. $I_{s,\text{peak}}$ with overcurrent protection by different C_n and P_n (a) Full Bridge, and (b) Half Bridge

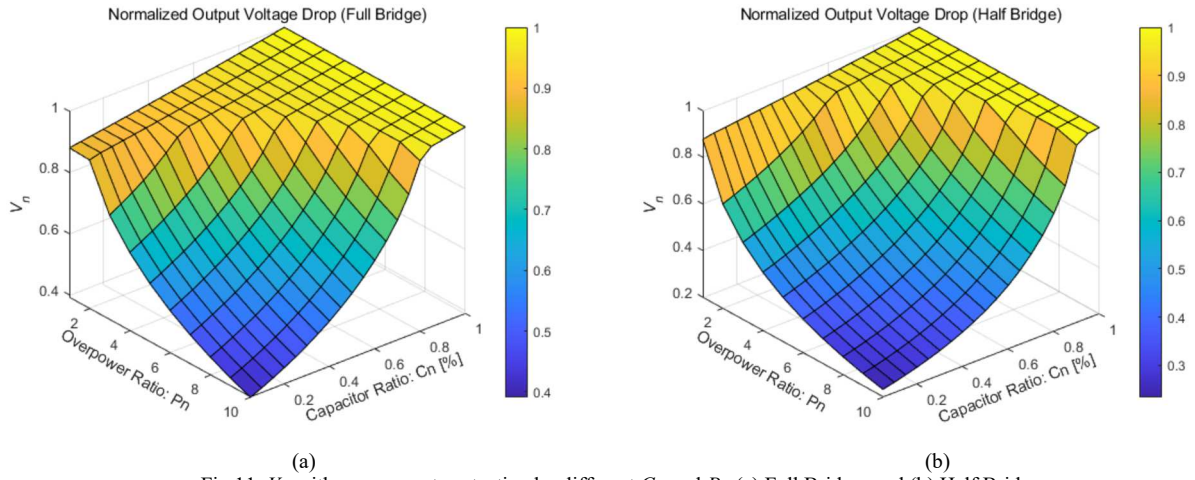


Fig. 11. V_n with overcurrent protection by different C_n and P_n (a) Full Bridge, and (b) Half Bridge

REFERENCES

- [1] A. Emadi, Advanced Electric Drive Vehicles. Boca Raton, FL, USA: CRC Press, Oct. 2014
- [2] M. Yilmaz and P. T. Krein, "Review of Battery Charger Topologies, Charging Power Levels, and Infrastructure for Plug-In Electric and Hybrid Vehicles," in IEEE Transactions on Power Electronics, vol. 28, no. 5, pp. 2151-2169, May 2013
- [3] M. Longo et al., "Recharge stations: A review," 2016 Eleventh International Conference on Ecological Vehicles and Renewable Energies (EVER), Monte Carlo, Monaco, 2016, pp. 1-8
- [4] S. K. Lee et al., "Cooperative decentralized peer-to-peer electricity trading of nanogrid clusters based on predictions of load demand and PV power generation using a gated recurrent unit model," IET Renewable Power Generation, 2021, pp. 3505-3523
- [5] I. Aghabali, J. Bauman, P. J. Kollmeyer, Y. Wang, B. Bilgin and A. Emadi, "800-V Electric Vehicle Powertrains: Review and Analysis of Benefits, Challenges, and Future Trends," in IEEE Transactions on Transportation Electrification, vol. 7, no. 3, pp. 927-948, Sept. 2021
- [6] P. SIGAL, "EV industry seen shifting to 800-volt architectures." Automotive News, Apr 2022, Accessed: Nov.2022 [Online]
- [7] M. M. Jovanović and B. T. Irving, "On-the-Fly Topology-Morphing Control—Efficiency Optimization Method for LLC Resonant Converters Operating in Wide Input- and/or Output-Voltage Range," in IEEE Transactions on Power Electronics, vol. 31, no. 3, pp. 2596-2608, March 2016.
- [8] W. Wang, W. Liu, W. Yao, L. Du, G. Chen and Z. Lu, "LLC Resonant Converter With Topology Morphing Rectifier for Wide Output Voltage Range Application," 2018 8th International Conference on Power and Energy Systems (ICPES), 2018, pp. 17-22
- [9] J. Wen, K. Sheng, J. Zhang, S. Yang and W. Jiang, "A Wide Output LLC Converter Based on Full Bridge and Half Bridge Topology Morphing Method Using Trajectory Transition," 2018 IEEE Energy Conversion Congress and Exposition (ECCE), 2018, pp. 6817-6821
- [10] Jiang, Linru, Xiaohong Diao, Yuanxing Zhang, Jing Zhang, and Taoyong Li. 2021. "Review of the Charging Safety and Charging Safety Protection of Electric Vehicles" World Electric Vehicle Journal 12, no. 4: 184.
- [11] K. -B. Park, B. -H. Lee, G. -W. Moon and M. -J. Youn, "Analysis on Center-Tap Rectifier Voltage Oscillation of LLC Resonant Converter," in IEEE Transactions on Power Electronics, vol. 27, no. 6, pp. 2684-2689, June 2012
- [12] K. -B. Park, B. -C. Kim, B. -H. Lee, C. -E. Kim, G. -W. Moon and M. -J. Youn, "Analysis and design of LLC resonant converter considering rectifier voltage oscillation," 2009 IEEE Energy Conversion Congress and Exposition, 2009, pp. 771-775
- [13] C. -Y. Chu et al., "Wireless Power Transfer System Design for Electric Vehicle Charging Considering A Wide Range of Coupling Coefficient Variation Depending on the Coil

- Misalignment," 2021 24th International Conference on Electrical Machines and Systems (ICEMS), Gyeongju, Korea, Republic of, 2021, pp. 732-737
- [14] D. Rothmund, G. Ortiz, T. Guillod and J. W. Kolar, "10kV SiC-based isolated DC-DC converter for medium voltage-connected Solid-State Transformers," 2015 IEEE Applied Power Electronics Conference and Exposition (APEC), Charlotte, NC, USA, 2015, pp. 1096-1103
 - [15] B. Yang, F. C. Lee and M. Concannon, "Over current protection methods for LLC resonant converter," Eighteenth Annual IEEE Applied Power Electronics Conference and Exposition, 2003. APEC '03., 2003, pp. 605-609 vol.2
 - [16] H. Bishnoi, S. Alvarez, G. Ortiz and F. Canales, "Comparison of Overload Protection Methods for LLC Resonant Converters in MVDC Applications," 2018 IEEE Energy Conversion Congress and Exposition (ECCE), 2018, pp. 3579-3586
 - [17] I. Cohen, "Series resonant circuit with inherent short circuit protection," United States Patent US6225862B1, 2001
 - [18] C. W. Tsang, M. P. Foster, D. A. Stone and D. T. Gladwin, "Analysis and Design of LLC Resonant Converters With Capacitor-Diode Clamp Current Limiting," in IEEE Transactions on Power Electronics, vol. 30, no. 3, pp. 1345-1355, March 2015
 - [19] R. L. Steigerwald, "A comparison of half-bridge resonant converter topologies," in IEEE Transactions on Power Electronics, vol. 3, no. 2, pp. 174-182
 - [20] A. Sankar, A. Mallik and A. Khaligh, "Extended Harmonics Based Phase Tracking for Synchronous Rectification in CLLC Converters," in IEEE Transactions on Industrial Electronics, vol. 66, no. 8, pp. 6592-6603, Aug. 2019
 - [21] Chaohui Liu, Jiabin Wang, K. Colombe, C. Gould and B. Sen, "A CLLC resonant converter based bidirectional EV charger with maximum efficiency tracking," 8th IET International Conference on Power Electronics, Machines and Drives (PEMD 2016), Glasgow, UK, 2016, pp. 1-6
 - [22] S. Zou, J. Lu, A. Mallik and A. Khaligh, "Bi-Directional CLLC Converter With Synchronous Rectification for Plug-In Electric Vehicles," in IEEE Transactions on Industry Applications, vol. 54, no. 2, pp. 998-1005, March-April 2018